Journal of Mechanics in Medicine and Biology
Vol. 13, No. 1 (2013) 1350020 (15 pages)

DOI: 10.1142/S0219519413500206

World Scientific
www.worldscientific.com

STRUCTURAL FEATURES AND MECHANICAL PROPERTIES OF PLLA/PEARL POWDER SCAFFOLDS

Y. S. LIU*, Q. L. HUANG*, Q. L. FENG*,§, N. M. HU† and O. ALBERT‡

*Laboratory of Advanced Materials
Department of Materials Science and Engineering
Tsinghua University, Beijing,100084, P. R. China

†Department of Orthopedics
General Hospital of Ningxia Medical University
Yinchuan 750004, P. R. China

‡ERC Advanced Investigator Grant Research Group at
the Institute for Physiological Chemistry
Mainz University Medical Center
Johannes Gutenberg University
Duesbergweg 6, D-55128 Mainz, Germany
§biomater@mail.tsinghua.edu.cn

Received 3 February 2012
Revised 27 May 2012
Accepted 11 September 2012
Published 19 October 2012

In order to improve the mechanical properties of scaffolds for bone tissue engineering, the present study aims to bring calcium carbonate ($CaCO_3$) with signaling molecules, namely pearl powder, into poly(L-lactic acid) (PLLA). PLLA/aragonite and PLLA/vaterite scaffolds were successfully fabricated by the freeze-drying method. Both composite scaffolds had a similar porous structure but a different saturated content of pearl powders. For both scaffolds, the porosity decreases and yield strength increases as pearl powder content increases. Introducing pearl powders into PLLA can improve the mechanical properties of the scaffolds. The porous structure plays a crucial role in the yield strength of pure PLLA scaffolds, whereas the yield strength of PLLA/pearl powder scaffolds mostly relies on pearl powder content.

Keywords: Composite scaffold; mechanical properties; pearl powder; aragonite; vaterite.

1. Introduction

Currently, many biomedical engineering projects involve some form of degradable, porous, and synthetic scaffold as a carrier, allowing cells to grow and proliferate.[1] In this aspect, composites of polymers and ceramics are suitable candidates for reinforcement. Thus, particle enhancement is seen as a good strategy to improve the mechanical stability of scaffolds.[2]

§Corresponding author.

The majority of all attempts to produce porous synthetic scaffolds focus on biodegradable polymers and bioactive ceramics.[3] The most common biodegradable polymer for scaffolds is poly(L-lactic acid) (PLLA). However, its mechanical performance is much lower than that of bone and the release of acidic degradation products could cause a strong inflammatory response.[2] Porous polymer scaffolds incorporated with bioactive ceramics, especially hydroxyapatite, offer sufficiently strong mechanical properties and reduce the risk of inflammatory reactions.[4] PLLA/nano-hydroxyapatite composites are promising porous bone substitutes which confer superior mechanical performance.[5] Nevertheless, despite its high mechanical performance and good biocompatibility, hydroxyapatite has an overly long degradation period.[6]

As a solution to this slow degradation problem, a feasible way is to introduce calcium carbonate ($CaCO_3$) with signaling molecules, namely pearl powders, into the synthetic scaffold structure instead of hydroxyapatite. $CaCO_3$ also shows good biocompatibility.[7,8] It is relatively less stable and dissolves more readily than calcium phosphate ($CaHPO_4$). On the other hand, signaling factors such as bone morphogenetic protein 2 (BMP-2) entrapped in scaffolds can increase bone formation. However, they can also be rapidly washed out in a short time and the high cost limits their field of applications.[9] Hence, it is desirable to fabricate porous composite scaffolds that offer sufficient mechanical performance as well as controlled signal factor release. The pearl is thus a promising choice.

The pearl is in fact, a most perfect combination of $CaCO_3$ and the organic matrix. It exhibits good bioactive characteristics and mechanical properties. Shen *et al.*[10] reported that pearl, acting as a natural carrier of bone growth factors, can stimulate osteoblast proliferation. Pearl powders significantly improve calcium bioresorption, based on the evaluation of bone formation in rats.[11]

There are two kinds of pearls in nature — aragonite and vaterite pearl. Aragonite pearl is composed of aragonite crystals and associated with an organic matrix (<5 wt%).[12] The inorganic component of lustrous pearls is constituted by aragonite crystals and is regarded as aragonite pearls.[13] Furthermore, our previous work confirmed that natural vaterite, combined with the organic matrix in pearl, shows high stability and enhanced mechanical properties, compared to pure inorganic vaterite.[14] The organic matrix in vaterite pearl is not exactly the same as in aragonite pearl, especially in a water-soluble matrix (WSM). Vaterite pearl contains more organic matrix than aragonite pearl.[14,15] Since nacre and aragonite pearl contain signal molecules in their WSM, we hypothesized that vaterite pearls also contain signal factors that could induce cells to adhere and proliferate. The addition of aragonite and vaterite pearl powder into a PLLA scaffold could be a convenient and effective way to prepare a porous scaffold with natural growth factors.

As per the norm for compressive mechanical testing of scaffolds, the peak compressive stress and compressive modulus were measured. Maximum stress is often closely linked with the preset proportion of compression and cannot accurately reflect mechanical compression.[16–19]

A significant difference to previous reported studies involving the measurement of mechanical properties is that the yield strength of scaffolds was also determined. Plastic deformation, in particular the initial yielding point, is sensitive to the local stress of various materials.[20] The yield strength and relative density of the porous metallic materials are used to determine the relationship between the compressive strength and density.[18] In the present study, we attempted to establish the relationship between yield strength and relative density in porous polymer materials. Another goal of the current study is to improve the bioactivity and mechanical properties of scaffolds by developing a composite scaffold of PLLA and pearl. Different amounts of aragonite pearl powder and vaterite pearl powder were added to PLLA scaffolds. The yield strength was measured to define correspondence with the relative density of scaffolds. Moreover, pure PLLA scaffolds were prepared to compare the mechanical properties with PLLA/pearl powder scaffolds.

2. Materials and Methods

2.1. *Materials*

Aragonite and vaterite pearls were harvested from Hyriopsis cumingii in Zhuji, Zhejiang province, China. The selected pearls were powdered to particles with size 10−50 μm. PLLA was purchased from a medical device company in Shandong, China and had an inherent viscosity of approximately 2.28 dL/g. 1,4-dioxane was purchased from Beijing Modern Eastern Fine Chemical Co. Ltd., China and was analytical grade.

2.2. *Fabrication of the scaffolds*

The PLLA scaffold was fabricated by the freeze-drying method. Briefly, PLLA was dissolved into 1,4-dioxane and stirred for 8 h by magnetic coupling at room temperature. The PLLA solutions had a final ratio of 2%, 3%, 4%, 5%, 6%, 7%, and 8% (wv^{-1}), respectively. The solutions were transferred into a flask and dispersed under sonication for 15 min. After this period, the mixture was placed into cylindrical molds. The molds were then frozen at −20°C for 24 h in a refrigerator. To sweep up the 1,4-dioxane, the mixture was freeze-dried at −50°C in vacuum condition for three days. To remove traces of organic solvent, the last step was to dry the samples in an oven at 40°C for five days. The porous pure PLLA scaffold was obtained and stored in a desiccator.

PLLA/aragonite was prepared by the following steps. First, the PLLA was dissolved into 1,4-dioxane to form a polymer 5% (wv^{-1}) solution. Then, the aragonite powder was added into the solution to form final ratios of 40%, 50%, 60%, 70%, and 80% (wv^{-1}) (on PLLA weight basis), respectively. The mixtures were stirred for 0.5 h and dispersed under sonication for 0.5 h. Thereafter, a part of the solutions were placed into cylindrical molds and followed the same freeze-drying process as described for the pure PLLA scaffold. The PLLA/vaterite scaffold was prepared by

the same freeze-drying method as the PLLA/aragonite scaffold. In order to determine the density of solid materials, the remaining solutions were cast on the surface of glass to form composite membranes. To obtain dense membranes, the casting solution was evaporated at 25°C for seven days.

2.3. *Morphologies of the scaffolds*

The appearances of the scaffolds were evaluated through scanning electron microscopy (SEM, FEI Quanta 200). To perform this, 10 samples were coated with gold for 7 min. The other five samples were observed without gold by SEM (Phenom Pro Suite, America) in order to maintain their original appearance.

Porosity, average pore size, and density of the scaffolds were measured by a mercury intrusion analyzer (Autopore IV 9510, America). Some sample characteristics could be measured and calculated directly, such as pore size distribution and median pore diameter. Measurements and analyses are presented as an arithmetic mean of three cylindrical specimens.

Density of solid membrane ρ_s is in triplicate and is computed using the following equation:

$$\rho_s = \frac{m}{\nu}, \tag{1}$$

where m is the weight of composite membrane with pearl powder and ν is the volume of the sample.

2.4. *Yield strength*

Mechanical properties of composite scaffolds were measured in compression mode with a Zwick Z005 universal testing machine at room temperature. All cylinder samples had a diameter of 8.44 mm and a height of 16 mm. Samples were compressed by a compressive force with a controlled speed of 1 mm min^{-1}. There was no definite point on the curve where elastic strain ended and plastic strain began. Therefore, the yield strength was chosen as the starting point of plateau stress in the stress−strain curve.

3. Results and Discussion

3.1. *Morphologies of the scaffolds*

Figure 1 shows the morphologies of the scaffolds. Generally, uniform structures were formed with large numbers of interconnected pores. Figures 2(a) and 2(b) show the same porous structure. These features reveal that PLLA/vaterite composite scaffolds, with the ratio of 50% and 60%, do not exhibit any substantial difference in the morphology. Figure 2(c) demonstrates a damaged porous structure with the composite scaffolds containing higher vaterite powder content (80%). In contrast, the walls of PLLA scaffolds with low pearl powder content were sufficient to support the

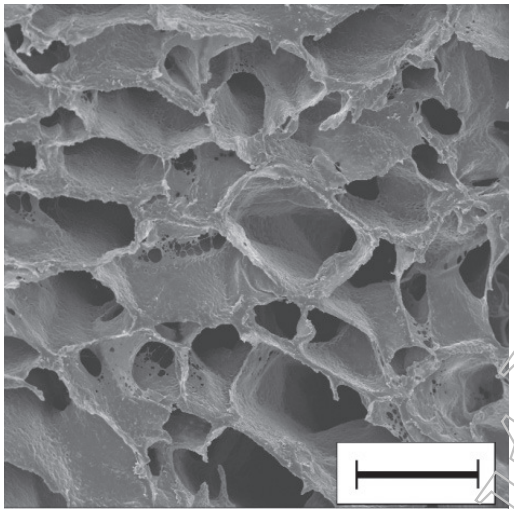

Fig. 1. Scanning electron micrographs of PLLA 5% (wv^{-1}). Scale bar is 100 μm.

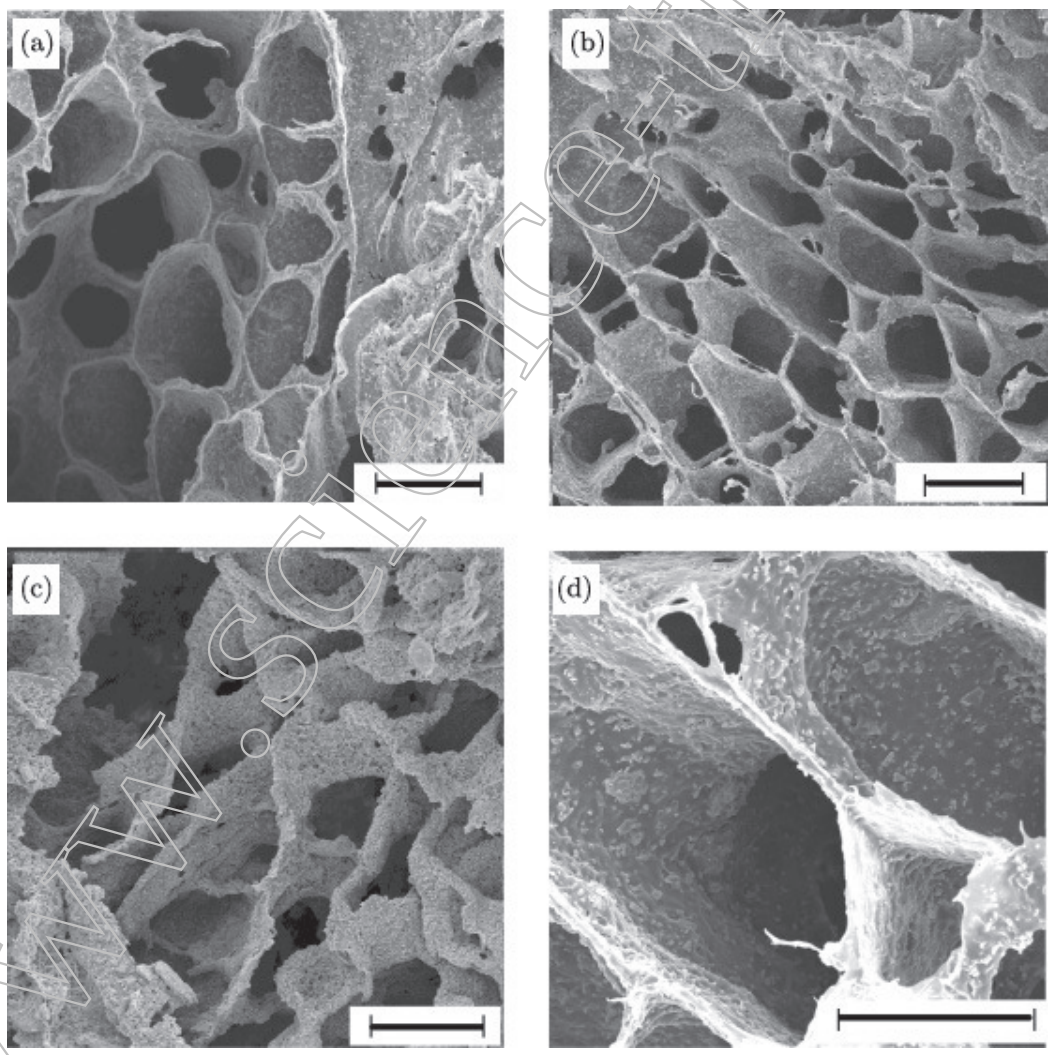

Fig. 2. Scanning electron micrographs of PLLA 5% (wv^{-1}) with different vaterite pearl powder contents (ww^{-1}) showing a porous structure. Scale bar is 100 μm. (a) PLLA/vaterite 60%; (b) PLLA/vaterite 70%; (c) PLLA/vaterite 80%; and (d) enlargement of PLLA/vaterite 60%.

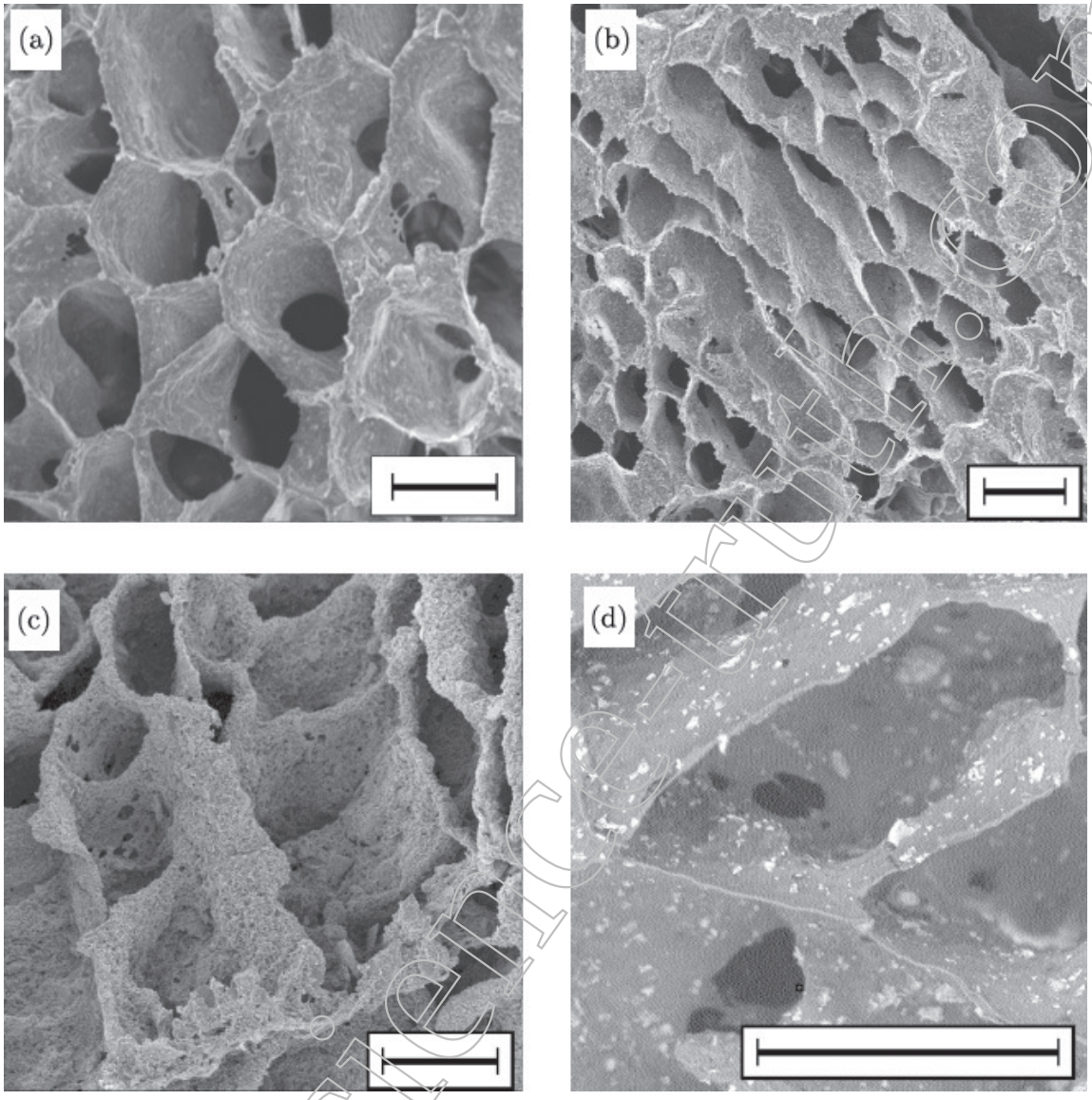

Fig. 3. Scanning electron micrographs of PLLA 5% (wv^{-1}) with different aragonite pearl powder contents (ww^{-1}) showing porous structure. Scale bar is 100 μm. (a) PLLA/aragonite 50%; (b) PLLA/aragonite 60%; (c) PLLA/aragonite 70%; and (d) magnification of PLLA/aragonite 60%.

porous structure. Figure 2(d) is the micrograph of the PLLA/vaterite composite scaffold and shows the distribution of pearl powder in the scaffold. It is apparent that there is a relatively high pearl powder content, as white spots are observed to cover the wall of the PLLA scaffold evenly. The morphologies of the PLLA/aragonite scaffolds are shown in Fig. 3. There are no visible differences between the two composite scaffolds. As shown in Fig. 3(c), collapses occured when the concentration of aragonite pearl powders was raised to 70%. Both composite scaffolds showed the same structure as PLLA, since most of the pearl powder was located on the PLLA wall and pore size was determined by the organic solvent via the freeze-drying method.

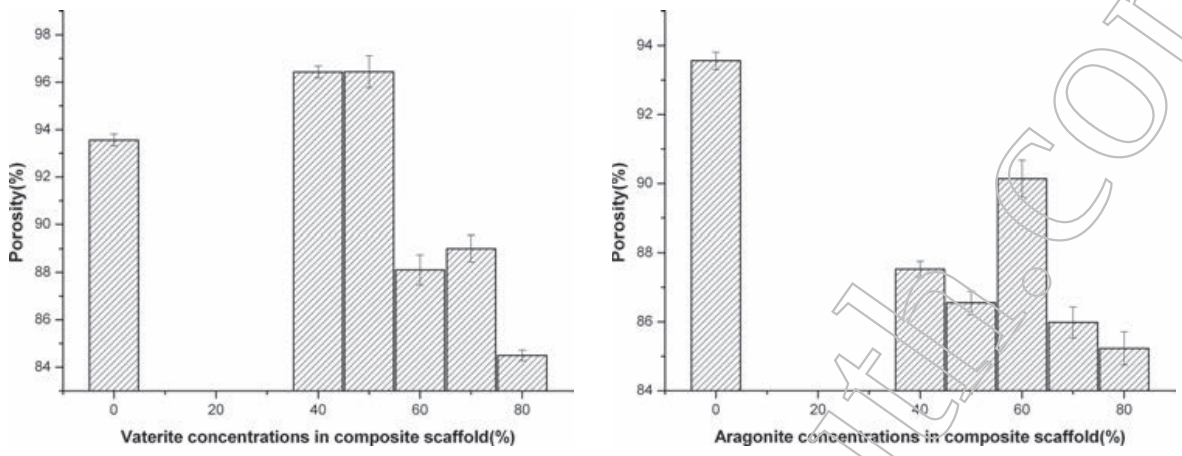

(a) (b)

Fig. 4. The relationship between porosity and pearl concentration in composite scaffolds. (a) Vaterite concentration in a composite scaffold and (b) aragonite concentration in a composite scaffold.

3.2. *Porosity*

In general, the average pore size of composite scaffolds was between 90 and 100 μm (result not shown) and each scaffold exhibited more than 83% porosity (Fig. 4). For scaffolds with 40% and 50% vaterite content, the porosity increased to 96%, similar to that of pure PLLA scaffold (93.56%). With increased pearl powder content, the porosity tends to decrease. A sudden increase in porosity was observed for the composite containing 70% vaterite. The scaffolds based on aragonite demonstrate a similar behavior; their porosity decreased as pearl powder content increased. An exception to this behavior was the 60% group, where a major porosity increase was noticeable. Such changes can happen when the concentration of pearl powders in the scaffold is raised up to 70% (vaterite) or 60% (aragonite). The pearl powder available in the scaffolds would reach a saturation level. In this specified state, pearl powder is more homogeneously distributed on the pore wall rather than outside the porous wall to maintain a more stable structure, resulting in a slight increase in porosity.

3.3. *Yield strength*

The stress–strain curves of PLLA/vaterite and PLLA/aragonite scaffolds are given in Fig. 5. When the concentration of pearl powders is increased, the stress of composite scaffold tends to increase. To estimate the mechanical performance of a scaffold, the yield strength was one of the primary parameters. [19] The yield strength was sensitive to the local stress of different materials.[18] In this work, the maximum stress of the linear part of stress–strain curve was chosen as the yield point. Figure 6 shows the stress–strain curves of a composite scaffold with 70% aragonite, in which

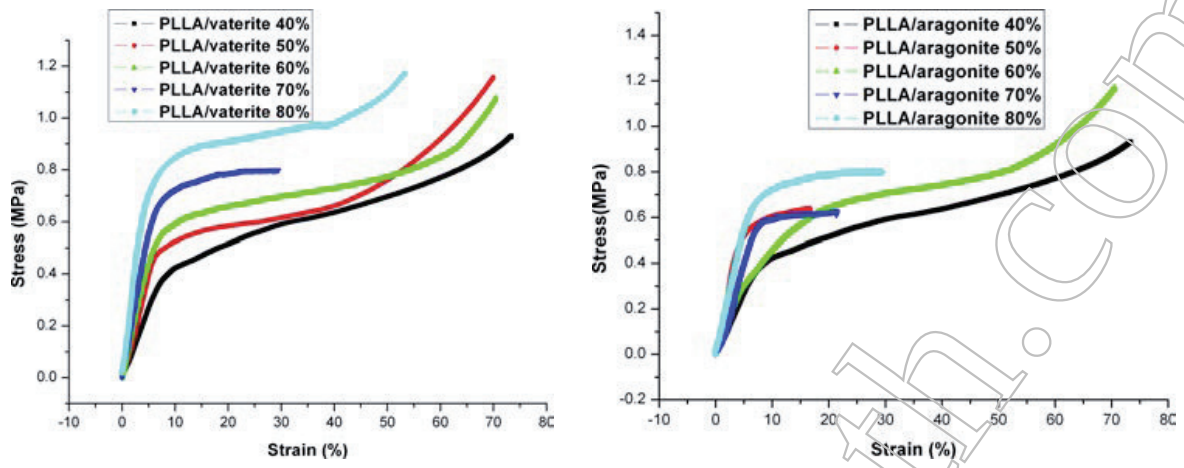

(a) (b)

Fig. 5. Stress–strain curves of composite scaffolds. (a) PLLA/vaterite scaffolds and (b) PLLA/aragonite scaffolds.

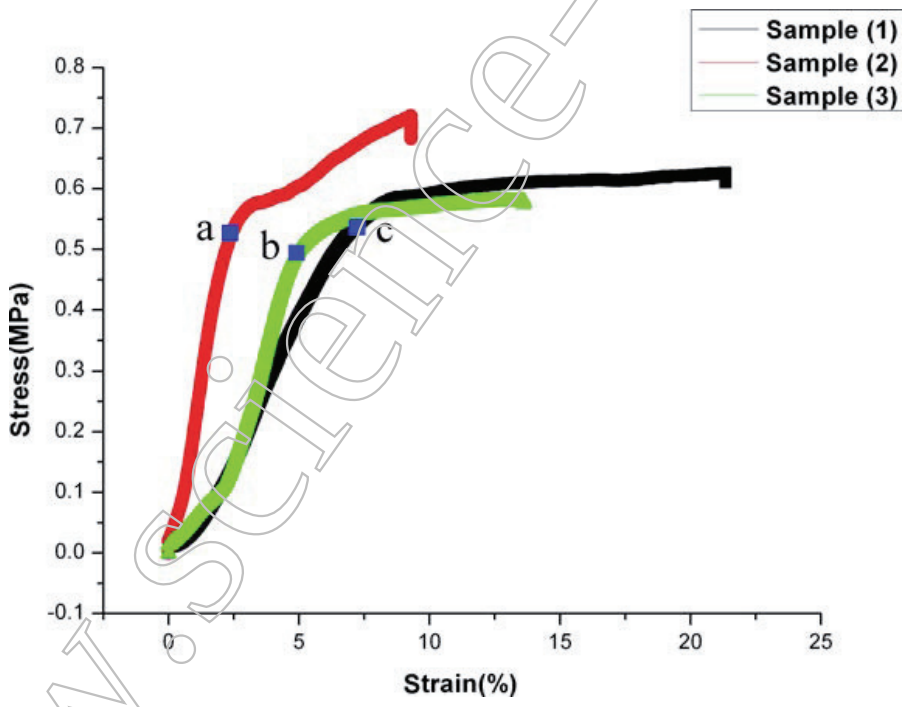

Fig. 6. Stress–strain curve of a composite scaffold with 70% aragonite.

points (a) –(c) are the highest points of the linear part of each stress–strain curve. The yield strength is 0.523 MPa, which is the arithmetic mean of three specimens.

The yield strength results of the PLLA/vaterite and PLLA/aragonite are presented in Fig. 7. Yield strength increases in the presence of pearl powders. It appears that the presence of pear powders positively correlates with the density of scaffolds and the yield strength of the material. With 40% vaterite, the yield strength is

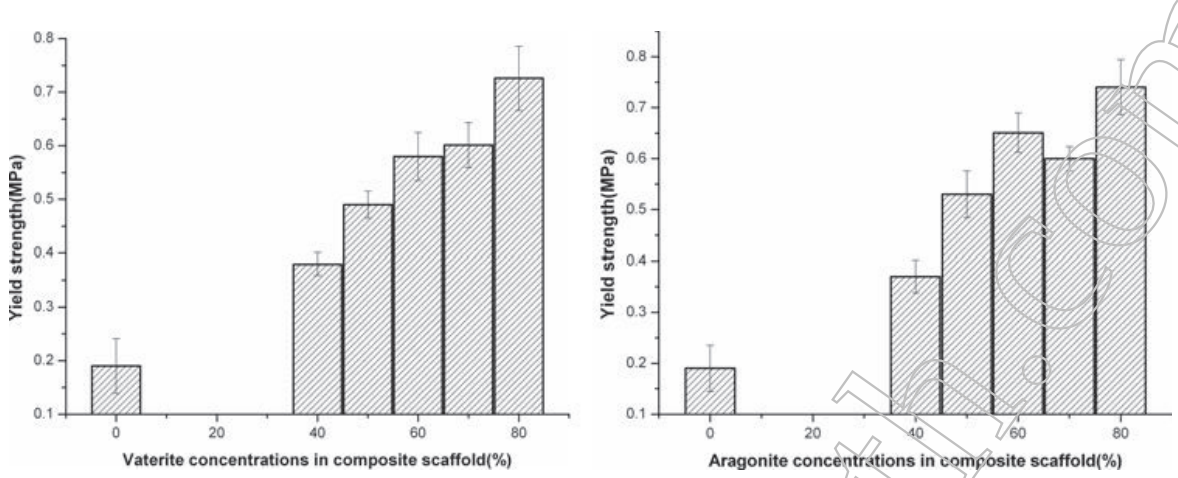

Fig. 7. The relationship between yield strength and pearl concentration in composite scaffolds.

doubled. With 80% vaterite, the yield strength is 3.5 times higher than that of pure PLLA. These results express that the increase of yield strength of the PLLA/pearl scaffold is derived from loaded pearl powders. The same trend is observed in the PLLA/aragonite scaffold. In this case, the maximum yield strength is nearly 2.5 times higher than that of PLLA. A similar result can be observed by comparing the left and the right sides of Fig. 7 for the same pearl powder concentration. These results demonstrate that two kinds of pearl powders act as defects in networks by damaging the continuity of PLLA structure. Nevertheless, the great strength of pearl powders causes an increase in the systematic mechanical properties as a whole. It can also be seen that for a scaffold with 60% aragonite, the yield strength increases suddenly and for a scaffold with 70% vaterite, the yield strength does not change. An explanation for this unexpected behavior can be that two composite scaffolds have reached a real saturation level. It means that on the pore walls, there is sufficient pearl powder for maximum coverage. It is these pearl powders that could prevent porous wall bending, which would result in the whole network undergoing deformation afterwards. In addition, because the hardness of aragonite is higher than vaterite, the yield strength of PLLA/aragonite increases more than vaterite.

To determine the principal source of mechanical properties, it is necessary to discuss the difference of the yield strength between a pure PLLA scaffold and a composite scaffold with pearl powders. Further studies on the yield strength of the two different systems were carried out. The main features of the pure PLLA scaffold include having a larger pore size about 100 μm and a higher porosity than the composite scaffolds. The yield strength depends not only on the material itself, but also on the structural characteristics such as porosity and pore size. For high porosity materials (>85%), it is possible that yield strength depends more on the relative density and structural features. Hence, the material itself is not the most important factor for yield strength.

Figure 8 shows that with increased PLLA content, the porosity of the scaffold tends to decrease. However, all scaffolds still have high porosity (at least 85%).

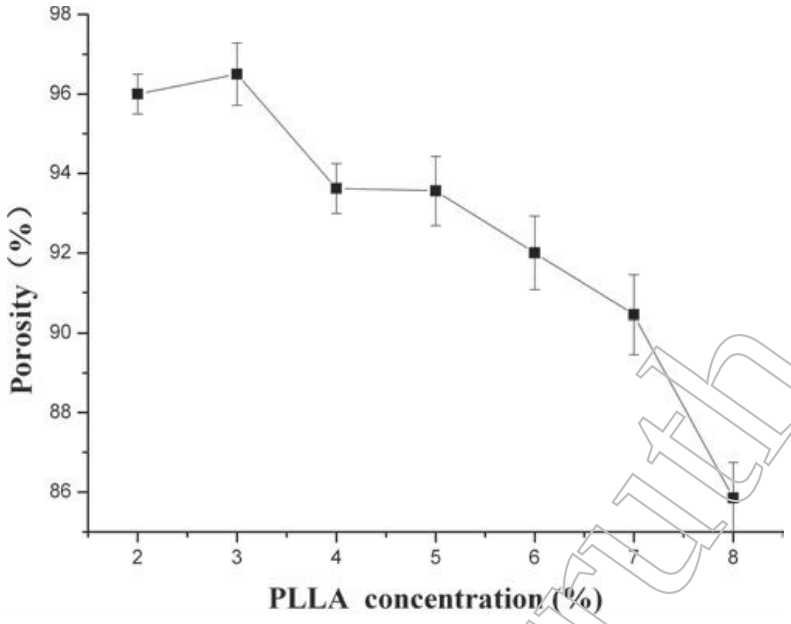

Fig. 8. The relationship between porosity and PLLA concentration in scaffolds.

The relative density ($\frac{\rho}{\rho_s}$) is the density of initial porous material ρ divided by the density of its cell solid ρ.[21]

Table 1 shows that with increasing PLLA concentration, the density of porous composite scaffolds rises. Relative density increases as well.

Figure 9 shows the relationship between the yield strength and the relative density of a pure PLLA scaffold. It is important to note that the relative density ranges from 0.2 to 0.9 and the yield strength rapidly increases with relative density, which can be described using a second order equation.

$$y = 0.0044 - 0.1408x + 0.7796x^2, \tag{2}$$

where x is the relative density and y the yield strength of scaffold. The coefficients are determined by the experiment.

Table 1. Comparison of part parameters of a pure PLLA scaffold.

PLLA concentration (%)	Density of porous PLLA scaffold $\rho \times 10^3$ (kg m^{-3})	Density of solid PLLA membrane $\rho \times 10^3$ (kg m^{-3})	Relative density ($\frac{\rho}{\rho_s}$)	Yield strength (MPa)
2	0.0293		0.201	0.0258
3	0.0475		0.325	0.0346
4	0.0573		0.392	0.0554
5	0.0857	0.1460	0.587	0.1900
6	0.0823		0.563	0.2530
7	0.1022		0.700	0.2994
8	0.1260		0.863	0.4590

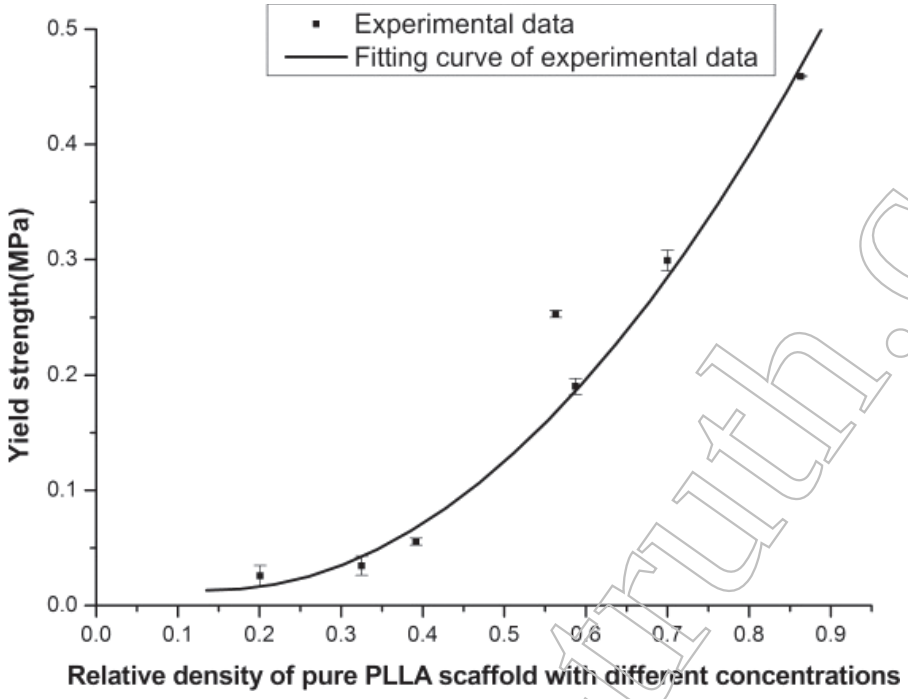

Fig. 9. The relationship between yield strength and relative density of pure PLLA scaffolds.

A PLLA porous scaffold has a typical foam structure. Earlier investigations have shown that porous metal exhibits many attractive characteristics, including enhanced compressive deformation with low density. The compressive property mostly depends on their relative densities.[21,22] Yield strength and relative density can be described by the following equation[23]:

$$\frac{\sigma}{\sigma_{y,s}} = C\left(\frac{\rho}{\rho_s}\right)^{3/2}\left(1+\left(\frac{\rho}{\rho_s}\right)^{1/2}\right) \quad \text{(open-cell model)}. \tag{3}$$

The coefficient C is estimated from the experimental data. The yield strength of porous material is represented by σ. While the yield strength of solid material, a constant value, is represented by $\sigma_{y,s}$. The open pore is a structure where the pores form interconnected network.[24] Equation (3) can be rearranged by expanding the equation

$$\sigma = C\sigma_{y,s}\left(\frac{\rho}{\rho_s}\right)^{3/2} + C\sigma_{y,s}\left(\frac{\rho}{\rho_s}\right)^{2} = C'\left(\frac{\rho}{\rho_s}\right)^{3/2} + C''\left(\frac{\rho}{\rho_s}\right)^{2}. \tag{4}$$

If we analyze Eq. (4) in the case where C' and C'' have small values, then the yield strength could be largely tied to relative material density.

Although PLLA is a polymer material and its deformation mechanism is different from metals, it is supposed that for maintaining high porosity, the yield strength of porous PLLA scaffolds depends more on the relative density and structural features rather than the solid material itself. Moreover, PLLA scaffolds present mostly a

circular-hole structure while observing them with SEM, so this result is consistent with the initial assumption of the two models. It is essential to compare Eqs. (2) and (4) to comprehensively understand the meaning of parameters as follows:

(1) The highest exponent from the Eqs. (2) and (4) is 2. The value of the maximum exponent may be governed by the deformation mode of individual cell structures or walls, such as yielding, bending, and buckling.[21] Therefore, the yield strength of porous PLLA scaffolds formally satisfies the law of the porous metal model. It could also be explained that in porous PLLA scaffolds, the maximum exponent is related to the porous structure rather than the solid material.
(2) All coefficients including the yield strength of the solid body were determined by the experiment. The coefficients of the fitted curve, $C' = -0.1408$ and $C'' = 0.7796$, have the same order of magnitude but of opposite algebraic sign. Thus, relative density may play a crucial role in evaluating the yield strength of a porous structure. Previous studies indicated that C' and C'' are constants for the geometric effect.[25] Therefore, all coefficients in the fitting equation contain the information of geometric factor and yield strength of the solid body.
(3) The exponent of x and $(\frac{\rho}{\rho_s})^{3/2}$ in Eqs. (2) and (4) are 1 and 1.5. Hence, the yield strength of PLLA scaffolds partly corresponds to the open-cell model of the porous metal equation. Due to limitations of the freeze-drying method, it is difficult to completely synthesize uniform pores and structure throughout the scaffold. The porous structures responsible for the yield strength of PLLA are a result of open pores as well as some closed pores.

From the analysis above, the porous metal model is deemed to offer an acceptable estimate for the yield strength of the porous PLLA scaffold. In contrast, PLLA scaffolds loaded with pearl powders are also a porous structure like pure PLLA. No substantial difference in the morphology and porosity between all kinds of scaffolds was observed. Relative density of this system is defined as $\frac{\rho}{\rho_s}$, where ρ_s is the body density after adding pearl powders and ρ is pore scaffold density after adding pearl powders. Table 2 shows that with increasing pearl powder concentration, the densities of porous composite scaffolds and solid materials similarly rise. However, the relative density tends to decrease.

Figure 10 demonstrates the relationship between the yield strength and relative density. Interestingly, the values of relative density are in the narrow range of 0.460 to 0.650. With increasing relative density, the yield strengths of two composite scaffolds similarly decreases. Such a descending trend provides conflicting information compared to the law of plastic deformation in composite scaffolds. The composite scaffold presented here does not fit the open-cell model, and its deformation mechanism is different to that of a pure PLLA scaffold. Thus, the porous structure in such networks may not play any significant role in yield strength. These results suggest that improvements to the mechanic performance of a scaffold are most

Table 2. Comparison of part parameters of composite scaffolds.

Pearl powder concentration	Density of porous material $\rho \times 10^3$ (kg m^{-3})	Density of composite membrane $\rho \times 10^3$ (kg m^{-3})	Relative density ($\frac{\rho}{\rho_s}$)	Yield strength (MPa)
vaterite 40%	0.1322	0.2039	0.6482	0.380
vaterite 50%	0.1551	0.2807	0.5525	0.490
vaterite 60%	0.1738	0.3525	0.4930	0.580
vaterite 70%	0.2169	0.4219	0.5141	0.601
vaterite 80%	0.2805	0.5779	0.4805	0.726
aragonite 40%	0.1360	0.2150	0.6314	0.370
aragonite 50%	0.2331	0.4335	0.5376	0.530
aragonite 60%	0.1461	0.3028	0.4825	0.651
aragonite 70%	0.2221	0.3700	0.6001	0.523
aragonite 80%	0.2791	0.5999	0.4650	0.740

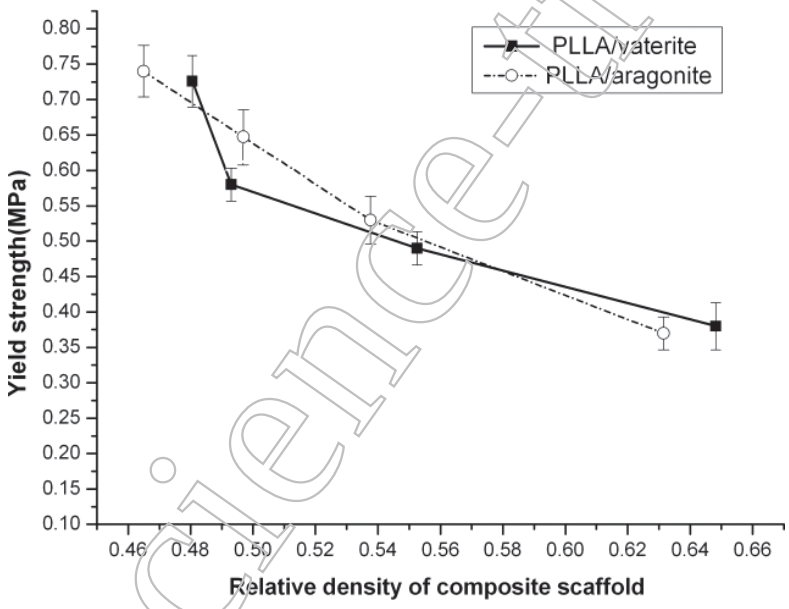

Fig. 10. The relationship between relative density and yield strength of PLLA/vaterite and PLLA/aragonite composite scaffolds.

reliant on the addition of pearl powders. This corresponds with the yield strength discussed above.

4. Conclusion

PLLA/aragonite and PLLA/vaterite scaffolds were fabricated by the freeze-drying method. Both composite scaffolds have a similar porous structure but a different saturated content of pearl powders. For composite scaffolds, the porosity decreases and the yield strength increases as pearl powder content increases. In the saturation

state, the porosity rebounds. Introducing pearl powders into PLLA markedly improves the mechanical properties of the scaffolds. The yield strength of the pure PLLA scaffold partly corresponds to the open-cell model, but composite scaffolds do not fit this model. The yield strength of the pure PLLA scaffold is determined by its porous structure, whereas composite PLLA/pearl powder scaffolds are dependent on the pearl powder added.

Acknowledgments

The authors are grateful for the financial support from the National Natural Science Foundation of China (51072090, 51061130554) and Doctor Subject Foundation of the Ministry of Education of China (20100002110074).

References

1. Yang XB, Whitaker MJ, Sebald W, Clarke NMP, Howdle SM, Shakesheff KM, Oreffo ROC, Human osteoprogenitor bone formation using encapsulated bone morphogenetic protein 2 in porous polymer scaffolds, *Tissue Eng* **10**(7–8):1137–1145, 2004.
2. Rezwan K, Chen QZ, Blaker JJ, Boccaccini AR, Biodegradable and bioactive porous polymer/inorganic composite scaffolds for bone tissue engineering, *Biomaterials* **27**(18):3413–3431, 2006.
3. Wang X, Song G, Lou T, Fabrication and characterization of nano-composite scaffold of PLLA/silane modified hydroxypatite, *Med Eng Phys* **32**(4):391–397, 2010.
4. Maquet V, Boccaccini AR, Pravata L *et al.*, Porous Poly(alpha-hydroxy acid)/Bioglass composite scaffolds for bone tissue engineering, *Biomaterials* **25**(18):4185–4194, 2004.
5. Gay S, Arostegui S, Lemaitre J, Preparation and characterization of dense nanohydroxyapatitie/PLLA compositeo, *Mater Sci Eng C Biomim Supram Syst* **29**(1):172–177, 2009.
6. Oonishi H, Kushitani S, Iwaki H, Comparative bone formation in several kinds of bioceramic granules, In: Wilson J, Hench LL, Greenspan D, eds. *Eighth Int Symp On Ceramics in Medicine*, Elsevier Science Ltd., Tokyo, 1995, pp. 137–144.
7. Vago R, Plotquin D, Bunin A, Sinelnikov I, Atar D, Itzhak D, Hard tissue remodeling using biofabricated coralline biomaterials, *J Biochem Biophys Methods* **50**(2–3):253–259, 2002.
8. Kim YW, Kim JJ, Kim YH, Rho JY, Effects of organic matrix proteins on the interfacial structure at the bone-biocompatible nacre interface *in vitro*, *Biomaterials* **23**(9):2089–2096, 2002.
9. Jha AK, Yang WD, Kim-Safran CB, Farach-Carson MC, Jia XQ, Perlecan domain I-conjugated, hyaluronic acid-based hydrogel particles for enhanced chondrogenic differentiation via BMP-2 release, *Biomaterials* **30**(36):6964–6975, 2009.
10. Shen YT, Zhu J, Zhang HB, Zhao F, *in vitro* osteogenetic activity of pearl, *Biomaterials* **27**(2):281–287, 2006.
11. Gao HY, Chen HJ, Chen WX, Tao F, Zheng YH, Jiang YM, Ruan HJ, Effect of nanometer pearl powder on calcium absorption and utilization in rats, *Food Chem* **109**(3):493–498, 2008.

12. Natoli A, Wiens M, Schröder H-C, Stifanic M, Batel R, Soldati AL, Jacob DE, Müller WEG, Bio-vaterite formation by glycoproteins from freshwater pearls, *Micron* **41**(4):359–366, 2010.
13. Ma YF, Gao YH, Feng QL, Characterization of organic matrix extracted from fresh water pearls, *Mater Sci Eng C* **31**(7):1338–1342, 2011.
14. Qiao L, Feng QL, Liu Y, A novel bio-vaterite in freshwater pearls with high thermal stability and low dissolubility, *Mater Lett* **62**(12–13):1793–1796, 2008.
15. Bedouet L, Rusconi F, Rousseau M, Duplat D, Marie A, Dubost L, Le Ny K, Berland S, Peduzzi J, Lopez E, Identification of low molecular weight molecules as new components of the nacre organic matrix, *Comp Biochem Physiol B* **144**(4):532–543, 2006.
16. Charles-Harris M, Valle SD, Hentges E, Bleuet P, Lacroix D, Planell JA, The mechanical and structural characterisation of completely degradable polylactic acid, *Biomaterials* **28**(30):4429–4438, 2007.
17. Tanaka SM, Li J, Duncan RL, Yokota H, Burr DB, Turner CH, Effects of broad frequency vibration as cultured osteoblasts, *J Biomech* **36**(1):73–80, 2003.
18. Zhang WX, Xu ZM, Wang TJ, Chen X, Effect of inner gas pressure on the elastoplastic behavior of porous materials: A second-order moment micromechanics model, *Int J Plast* **25**(7):1231–1252, 2009.
19. Ramtani S, Takahashi-Iniguez Y, Helary C, Geiger D, Guille MMG, Mechanical behavior under unconfined compression loadings of dense fibrillar collagen matrices mimetic of living tissues, *J Mech Med Biol* **10**(1):35–55, 2010.
20. Cao AJ, Ma E, Sample shape and temperature strongly influence the yield strength of metallic nanopillars, *Acta Mater* **56**(17):4816–4828, 2008.
21. Hakamada M, Asao Y, Kuromura T, Chen YQ, Kusuda H, Mabuchi M, Density dependence of the compressive properties of porous copper over a wide density range, *Acta Mater* **55**(7):2291–2299, 2007.
22. Goodall R, Marmottant A, Salvo L, Mortensen A, Spherical pore replicated microcellular aluminium: Processing and influence of properties, *Mater Sci Eng A* **465**(1–2):124–135, 2007.
23. Gibson LJ, Ashby MF, *Cellular Solids: Structure and Properties*, Cambridge University Press, 1999.
24. Veyhl C, Belova IV, Murch GE, Fiedler T, Finite element analysis of the mechanical properties of cellular aluminium based on micro-computed tomography, *Mater Sci Eng A* **528**(13–14):4550–4555, 2011.
25. Liu PS, Failure by buckling mode of the pore-strat for isotropic three-dimensional reticulated porous metal foams under different compressive loads, *Mater Des* **32**(6):3493–3498, 2011.